Cellular ceramics from emulsified suspensions of mixed particles

Suelen Barg, Bernard P. Binks, Hailing Wang, Dietmar Koch, Georg Grathwohl

Angaben zur Veröffentlichung / Publication details:

Barg, Suelen, Bernard P. Binks, Hailing Wang, Dietmar Koch, and Georg Grathwohl. 2012. "Cellular ceramics from emulsified suspensions of mixed particles." *Journal of Porous Materials* 19 (5): 859–67. https://doi.org/10.1007/s10934-011-9541-2.

Cellular ceramics from emulsified suspensions of mixed particles

Suelen Barg · Bernard P. Binks · Hailing Wang ·
Dietmar Koch · Georg Grathwohl

Abstract In this work concentrated alumina suspensions have been emulsified with decane using silica nanoparticles of a range of hydrophobicities as stabiliser giving rise to novel porous ceramic materials. The materials are characterized by open porosities between 49 and 61% and average cell sizes between 18 and 25 μm. Comparison with surfactant-stabilized emulsified suspensions is given. In particular, high temperature strength is a key property of the particle-stabilized materials.

Keywords Emulsified suspension · Pickering emulsion · Cellular ceramic

1 Introduction

Nowadays macroporous ceramics with cellular microstructures find applications in a wide range of technological fields. The combination of ceramic materials and controlled porosity parameters results in specific properties, making cellular ceramics functional as filters, structural materials, insulators, catalytic supports, electrodes, burners and biomaterials, amongst others [1–9]. The tailored microstructures required by the specific application have to be realized by adjusting the synthesis parameters and the processing routes [10, 11]. The use of emulsions as templates or intermediates has been shown to be a promising approach for the fabrication of porous ceramics in recent years. The stabilization of the liquid–liquid interface, however, is a key issue with respect to the stability and microstructural formation of the materials.

Surface-active molecules like long chain surfactants can provide enhanced stability to emulsions. Ordered macroporous inorganic structures have been produced by fractionating surfactant-stabilized emulsions produced with sol–gel reactants [12]. Some authors have produced polymeric porous materials by different emulsion template methods and subsequently transformed them into organic porous materials by immersion in sol–gel solutions containing the metal oxide precursors [13–15]. Recently, cellular ceramics of tailored microstructural features and excellent mechanical properties have been developed by the direct foaming of surfactant-stabilized emulsified particle suspensions [16–19].

More than one century ago Pickering showed that particles adsorbed at a liquid–liquid interface can lead to very stable emulsions (so-called Pickering emulsions) [20]. In contrast to the dynamic adsorption and desorption of surfactants, colloidal particles may adsorb irreversibly to the interface providing a higher stability against coalescence and Ostwald ripening. Following this idea, particle-stabilized emulsions have been used as intermediates for the production of macroporous organic–inorganic [21–23] and inorganic materials [24–27]. For emulsions stabilized by

S. Barg (✉)
CASC, Department of Materials, Imperial College London,
London SW7 2AZ, UK
e-mail: suelen.barg@imperial.ac.uk

S. Barg · H. Wang · D. Koch · G. Grathwohl
Keramische Werkstoffe und Bauteile, University of Bremen,
28359 Bremen, Germany

B. P. Binks (✉)
Surfactant and Colloid Group, Department of Chemistry,
University of Hull, Hull HU6 7RX, UK
e-mail: b.p.binks@hull.ac.uk

D. Koch
Deutsches Zentrum für Luft- und Raumfahrt e.V. in der
Helmholtz-Gemeinschaft, Institut für Bauweisen- und
Konstruktionsforschung, 70569 Stuttgart, Germany

surfactant, the hydrophile-lipophile balance (HLB) number is important in selecting the optimum emulsifier. In the case of particle-stabilised emulsions, the wettability of the particle at the oil–water interface, as judged by the three-phase contact angle, is crucial in favouring adsorption at the liquid–liquid interface. Binks et al. [24, 25] have developed a method for the preparation of porous silica from silica nanoparticle-stabilized emulsions, where the nanoparticle wettability is varied in a wide range by surface chemical treatment (silanization). Macroporous ceramics have also been produced by the in situ modification of the hydrophobicity of colloidal particles with the use of short chain amphiphilic molecules. As the particles are initially hydrophilic they can be homogeneously dispersed up to high concentrations in the water-based suspension. Closed cells provided by the irreversibly adsorbed particle shell are predominant [26, 27].

In this article, we present a new method for the fabrication of cellular ceramics based on emulsified suspensions stabilized by alumina (Al_2O_3) and silica (SiO_2) aggregates. In contrast to previous work, no surface-active molecules are required for emulsion stabilisation. The influence of the silica particle wettability on the configuration of the emulsified suspensions as well as on the microstructure of the porous ceramics prepared is discussed. The effect of particle or surfactant stabilization on the processing of the materials is also compared. Finally, envisaging the possible application fields of the novel materials, their compressive strength at high temperature (1,500 °C) is investigated.

2 Experimental section

2.1 Processing route

The cellular inorganic materials developed in this work were processed in four steps as illustrated in Fig. 1, using either nanoparticles or surfactant for emulsion stabilisation. The first one was the preparation of a stable Al_2O_3 powder (Alcoa CT 3000SG, d_{50} of 500 nm, specific surface area of 7.5 m^2/g) suspension in water. For the production of mixed particle-stabilized emulsified suspensions, Pa-Em, the Al_2O_3 powder was added to water containing HCl (Roth) at a concentration of 2 M for electrostatic stabilization. The acidic pH = 5 provided by the addition of HCl results in particles becoming positively charged. In the case of surfactant-stabilized emulsified suspensions, Su-Em [16, 17], Al_2O_3 powder was added stepwise to deionised water containing a polyacrylate (0.74 wt% relative to alumina), commercially available as Dolapix CE-64 (Zschimmer & Schwarz), as an electrosteric dispersion agent resulting in a highly negative surface charge on the alumina particles at pH = 9. Dispersion and homogenization was carried out in a laboratory mixer (Dispermat LC, VMA Getzmann) at 2,500 rpm for 20 min at room temperature. The charge on alumina particles was adjusted to be either positive to promote interaction with the silica nanoparticles or negative to avoid their interaction with the anionic surfactant.

For the preparation of Pa-Em, decane (>99%, Fluka) was dispersed in the Al_2O_3 suspension with the addition of

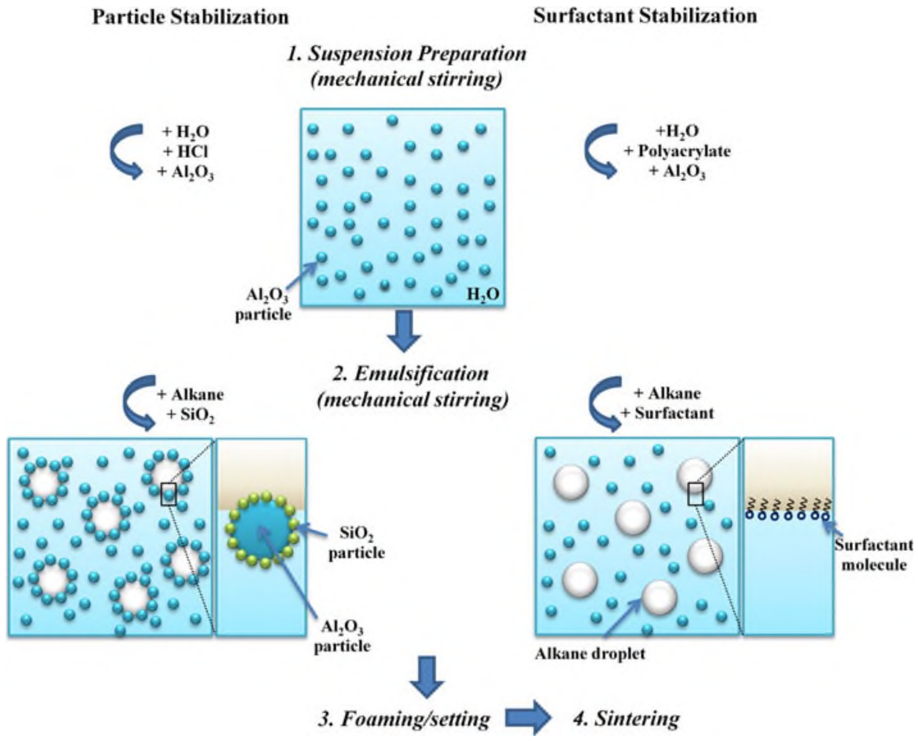

Fig. 1 Schematic illustration of the processing route for (*left*) mixed particle- stabilised emulsified suspensions, Pa-Em, and (*right*) surfactant-stabilized emulsified suspensions, Su-Em

SiO_2 nanoparticles as a powder of different hydrophobicity (as provided by supplier), possessing between 100% SiOH (hydrophilic) and 15% SiOH (very hydrophobic) groups (Wacker-Chemie, primary particle diameter 20–30 nm, surface area 200 $m^2\ g^{-1}$), by mechanical stirring. Starting from purely hydrophilic silica, particles were made progressively hydrophobic by reaction with dichlorodimethylsilane in the presence of water, with either the concentration of silane reagent or the reaction time varying. At pH 5, Al_2O_3 and SiO_2 particles are positively and negatively charged, respectively. The opposite charges as well as the difference in size between these particles promote their attraction resulting in heteroaggregation [28]. This leads to a combined particle stabilization due to the attachment of the Al_2O_3-SiO_2 aggregates around the oil drops in water. On the other hand, for Su-Em, the stabilization of the decane droplets was achieved by the addition of sodium lauryl sulphate SLS (BASF, Lutensit AS 2230), as anionic surfactant and emulsifier. Here, the Al_2O_3 particles and the surfactant molecules are both negatively charged in order to avoid their interaction. Emulsification is aided by mechanical stirring for 2.5 min. This process was carried out under reduced pressure (10 kPa) to avoid air bubble incorporation.

Subsequently, in surfactant-stabilized emulsified suspensions, foaming was provided by alkane droplet evaporation. If the physical conditions are favourable foaming can lead to a time-dependent growth of the wet foam [16, 17, 19]. Meanwhile setting of the structures took place due to the evaporation of the solvents (water and decane). During this process the alumina particles pack together ensuring the materials' green stability. Emulsified suspensions stabilized by nanoparticles transit into green foams in a similar way as described for surfactant-stabilized systems, without foaming however, since the stabilized bubbles are more stable against growth. After 24 h, the Pa-Em and Su-Em-based samples were sintered at 1,550 °C for 2 h in an electrical furnace. Heating and cooling rates of 3 and 5 K/min. respectively were applied. The compositions and processing conditions for the materials prepared in this work are summarized in Table 1.

2.2 Characterization

Immediately after emulsification, the conductivity of the emulsified suspensions was measured using a LF3000 microprocessor conductivity meter (WTW, Germany) at 20 °C. The linear shrinkage ($d - d_o/d_o$) of the porous solids was determined from the initial diameter just after preparation, d_o, and the diameter, d, after setting only or after setting and sintering for the linear shrinkage after setting and sintering, respectively.

Scanning Electron Microscopy, SEM, (Camscan 24, Cambridge, UK) was used for the microstructural analysis of the sintered cellular structures. Cell sizes were measured from planar sections with the linear intercept method using the software Linear Intercept (TU Darmstadt). Strut thickness was measured from planar sections with the help of an image analysis program (Axio Vision). The characteristic cell and strut sizes (d_{90}, d_{50} and d_{10}) were determined from the cumulative cell size distribution curves of three pictures taken from different regions of the sample. The total and open porosity of the materials was calculated using the Archimedes method considering three different weights of the specimen: m_1 (dry specimen weight), m_2 (weight of the specimen under water) and m_3 (weight of the wet specimen).

Thermal diffusivity was measured by the laser flash method (Netzsch, LFA 457 Micro Flash). High temperature compression tests were performed using a Zwick 1465 testing instrument. The testing temperature of 1,500 °C was achieved within 20 min induced by inductive heating. After 5 min of dwelling time the cylindrical specimens of

Table 1 Composition of samples prepared

Sample codename	Al_2O_3 content in suspension/ vol.%	Silica or surfactant (in emulsion)/ vol.%	SiOH on silica surface[a]/%	Decane content/ vol.%	Stirring velocity/rpm
Pa-Em-15% SiOH	35	0.11	15	50	2,500
Pa-Em-30% SiOH	35	0.11	30	50	2,500
Pa-Em-50% SiOH	35	0.11	50	50	2,500
Pa-Em-60% SiOH	35	0.11	60	50	2,500
Pa-Em-70% SiOH	35	0.11	70	50	2,500
Pa-Em-80% SiOH	35	0.11	80	50	2,500
Pa-Em-100% SiOH	35	0.11	100	50	2,500
Su-Em-1	35	0.11	–	50	800
Su-Em-2	35	0.11	–	50	2,500
Su-Em-3	42	0.11	–	50	800

[a] As provided by Wacker-Chemie

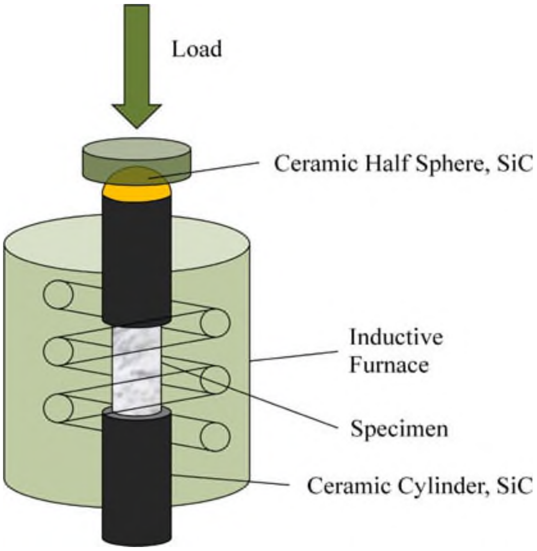

Fig. 2 Schematic illustration of the porous solid testing rig

either 15 or 25 mm diameter were loaded in displacement control with a speed of 0.5 mm/min. The first significant load drop indicated compressive failure. The sketch of the testing rig is shown in Fig. 2.

3 Results

3.1 Mixed particle-stabilized emulsified suspensions, Pa-Em

The control of the residual SiOH content on the SiO_2 particle surfaces leads to particles of tunable wettability. Emulsification with SiO_2 particles containing 15–80% SiOH groups resulted in very stable emulsified suspensions where no phase separation of either oil or water was observed. The use of completely hydrophilic SiO_2 particles possessing 100% SiOH as emulsifier was not effective in promoting total emulsification of the dispersed phase and some phase separation (excess oil) was observed.

The conductivity of Pa-Em emulsified with SiO_2 particles of different SiOH content on their surfaces is shown in Table 2. The emulsified suspensions stabilized by particles are characterized by high conductivities beyond 1,800 µS/cm. This, along with the drop test results, gives evidence for the formation of oil-in-water emulsified suspensions using silica particles of any hydrophobicity.

The control of the particle wettability in particle-stabilized emulsions is known to lead to an exchange of the dispersed and the continuous phase (phase inversion). Water-toluene emulsions stabilized by SiO_2 particles alone undergo phase inversion from water-in-oil to oil-in-water for particles possessing >50% SiOH on their surfaces (more hydrophilic) [25, 29]. In contrast, our results for Al_2O_3-SiO_2 aggregates as emulsion stabilizers present a different trend when compared to the stabilization by such SiO_2 particles alone. The Al_2O_3-SiO_2 aggregates most probably exhibit a changed contact angle with the oil–water interface which is different to either particles alone allowing the preference for oil-in-water emulsions in the whole range of particle wettability.

The production of stable emulsified suspensions is followed by their transition into green solid foams before sintering (Fig. 3). This transition is enabled due to evaporation of the oil phase and concurrent drying (water evaporation) of the emulsified suspensions. During this stage the particles pack together resulting in shrinkage of the foams. The green (non-sintered) foams undergo linear shrinkages between 3.2 and 3.7% after 24 h setting (Table 2). Further consolidation of the foams is achieved by sintering at 1,550 °C where the diffusion processes lead

Table 2 Conductivity of Pa-Em (particle) and linear shrinkage of solid foams (after setting for 24 h and after sintering at 1,550 °C for 2 h) as a function of SiOH content of SiO_2 particles

Sample codename	Conductivity/ µS cm^{-1}	Linear shrinkage after setting/%	Linear shrinkage after sintering/%
Pa-Em-15% SiOH	1,817	3.70	19.30
Pa-Em-30% SiOH	1,840	3.20	18.47
Pa-Em-50% SiOH	1,861	3.18	19.02
Pa-Em-60% SiOH	1,835	3.57	18.78
Pa-Em-70% SiOH	1,850	3.31	19.15
Pa-Em-80% SiOH	1,848	3.50	18.62
Pa-Em-100% SiOH	1,860	3.70	19.30

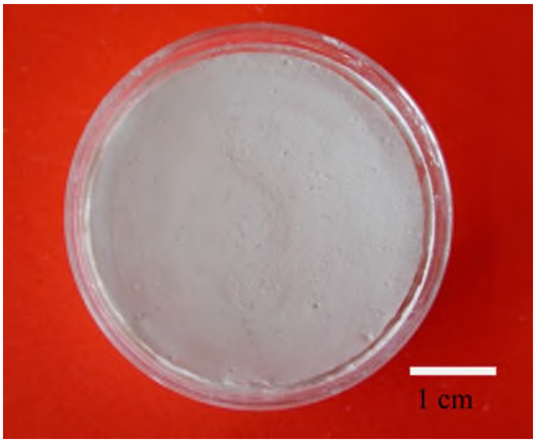

Fig. 3 Crack-free green solid foam resulting from a nanoparticle-stabilized emulsified suspension, Pa-Em

to sintering contacts and grain growth. The materials undergo a total shrinkage between 18.5 and 19.3% (Table 2). The final porous solid foam microstructures and the corresponding porosity parameters as a function of the silanol content on silica particles are shown in Figs. 4 and 5, respectively.

The materials produced using silica particles possessing between 15 and 80% SiOH yield similar porosity parameters. As the dispersed phase volume fraction was kept constant at 50 vol.% the materials present total porosities between 62.2 and 63.6%. A closed porosity of approximately 2–3% is found in the materials as a result of enclosed pores in the struts. In the case of 100% SiOH particles, the total porosity corresponds to 50.6% as a result of the incomplete emulsification of the dispersed phase. Neither the cell size distribution, Fig. 5a nor the strut thickness, Fig. 5b, shows any significant variation with the silanol content below 80% SiOH. The materials are characterized by an average cell diameter between 18 and 25 µm and average strut thickness between 2.7 and 3.6 µm.

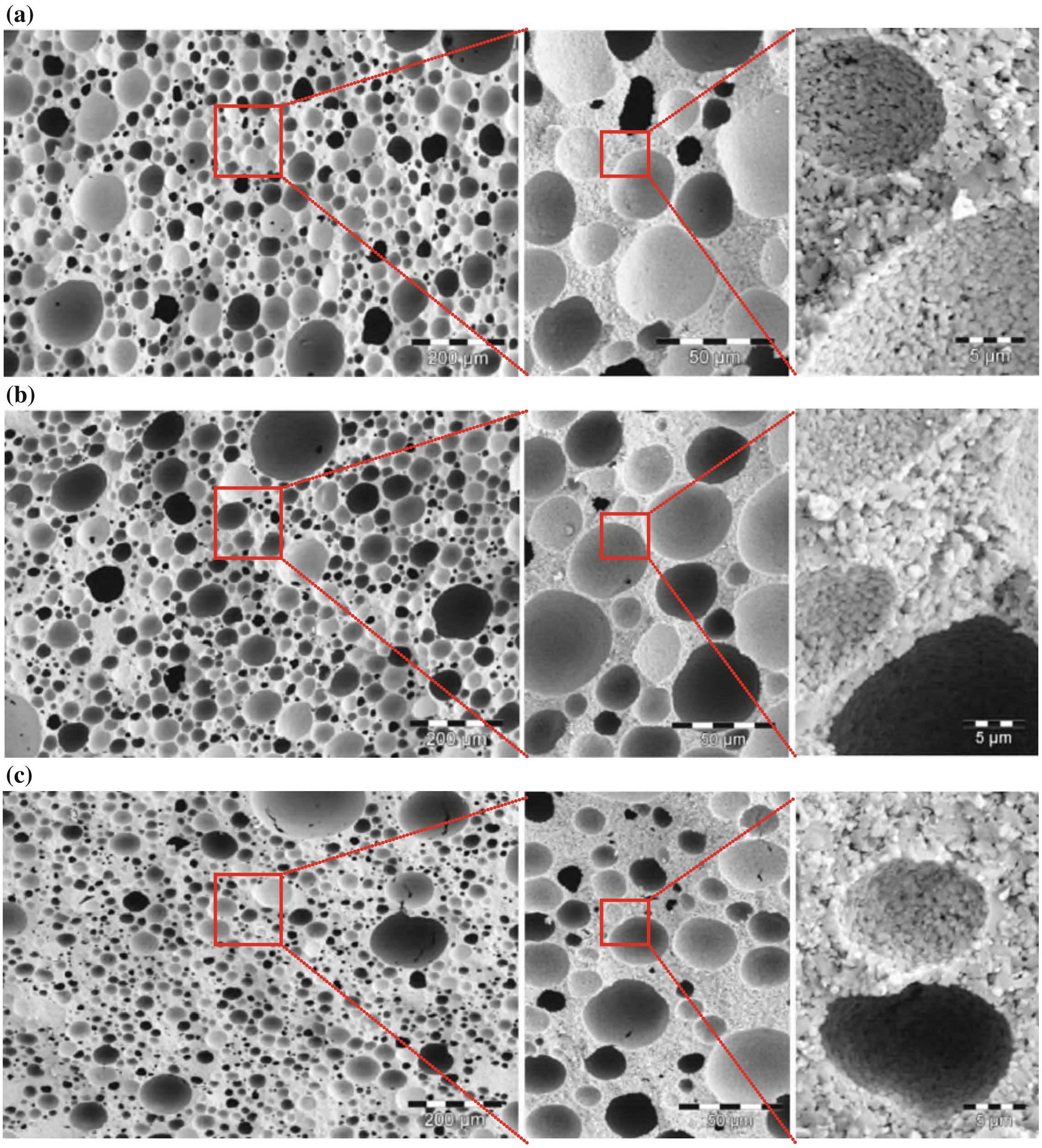

Fig. 4 SEM microstructures of sintered foams produced from Pa-Em (composition in Table 1) with different residual SiOH content on SiO_2 particles. **a** Pa-Em-15% SiOH at three magnifications, **b** Pa-Em-50% SiOH, **c** Pa-Em-100% SiOH

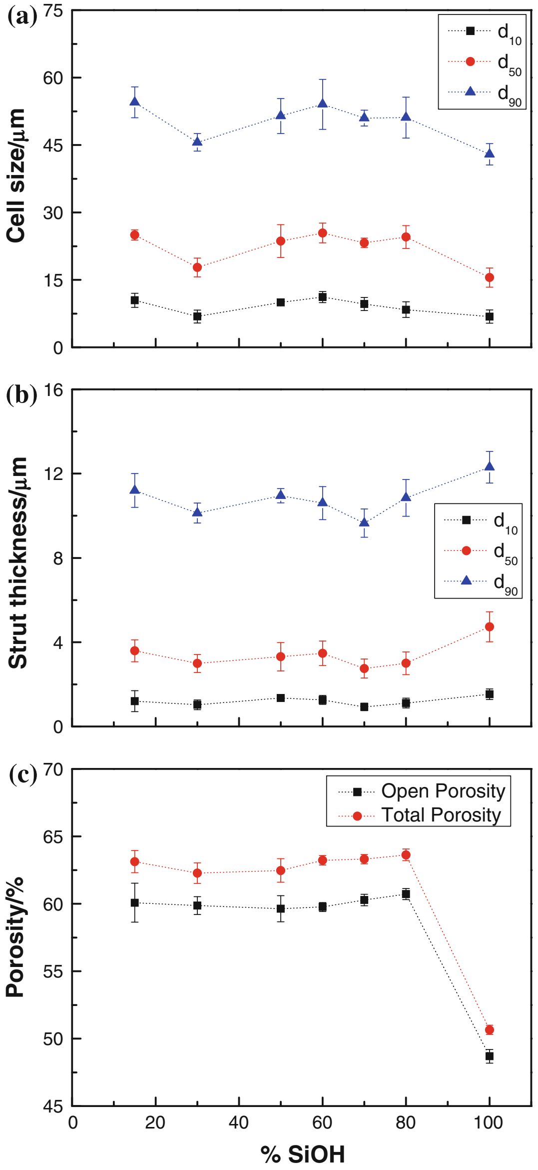

Fig. 5 Porosity parameters of sintered foams of Pa-Em. **a** Cell size, **b** strut thickness, **c** total and open porosities as a function of residual SiOH content on SiO_2 particles

For 100% SiOH particles, however, the lower concentration of cells leads to a larger distance between them and consequently wider struts.

3.2 Particle, Pa-Em, versus surfactant, Su-Em, stabilized emulsified suspensions

The way precursor droplets are stabilized in the emulsified suspensions influences the microstructure of the cellular ceramics formed afterwards. Using an anionic surfactant in place of silica particles allows lower oil–water interfacial tensions to be attained and smaller oil drop sizes after emulsification. Depending on the Al_2O_3 particle content in suspension and the emulsification stirring velocity average droplet sizes of 18 µm for Su-Em-1, 15 µm for Su-Em-3 and 6.5 µm for Su-Em-2 can be produced. The conductivities of surfactant-stabilized emulsified suspensions of different compositions are given in Table 3. They are characterized by oil-in-water morphology as in the case of particle stabilization but with lower conductivity values.

Table 3 Conductivity of Su-Em (surfactant) and linear shrinkage of solid foams (after setting for 24 h and after sintering at 1,550 °C for 2 h) for different compositions

Sample codename	Conductivity/ µS cm^{-1}	Linear shrinkage after setting/%	Linear shrinkage after sintering/%
Su-Em-1	897	0.25	13.33
Su-Em-2	927	1.85	14.82
Su-Em-3	930	0.66	14.55
Pa-Em-80% SiOH	1,848	3.50	18.62

Foams produced from Pa-Em-80% SiOH are given for comparison

Surfactant-stabilized foams presented a total linear shrinkage after sintering (13.3–14.8%) lower than particle-stabilized foams (18.6%). During the transition of the emulsified ceramic particle suspension into the wet foam, bubbles are formed as the decane droplets evaporate. This along with the concurrent drying of the suspension gives rise to green foams. The stabilization of the droplet interfaces influences this process. When the alkane droplets are stabilized by surfactant molecules, they expand during evaporation depending on the conditions and coalescence can occur. This has been observed via fluorescence microscopy [16].

In the case of particle-stabilized interfaces, expansion and destabilization mechanisms are less likely to take place. Bubble expansion counterbalances particle densification during water evaporation leading to lower shrinkage in surfactant-stabilized systems during setting. Further on, the growing bubbles compress the particle suspension localized between them resulting in extra aid in the densification of the cell walls and struts during drying. Denser struts during setting lead to reduced densification after sintering.

By adjusting the processing conditions, in this case the emulsification stirring velocity and the particle content in suspensions, the droplet size and the foaming of Su-Em can be controlled. Consequently, cellular ceramics of different porosity parameters can be achieved as seen in Figs. 6 and 7. The processing and microstructure control of these materials has been outlined in more detail elsewhere [16–19].

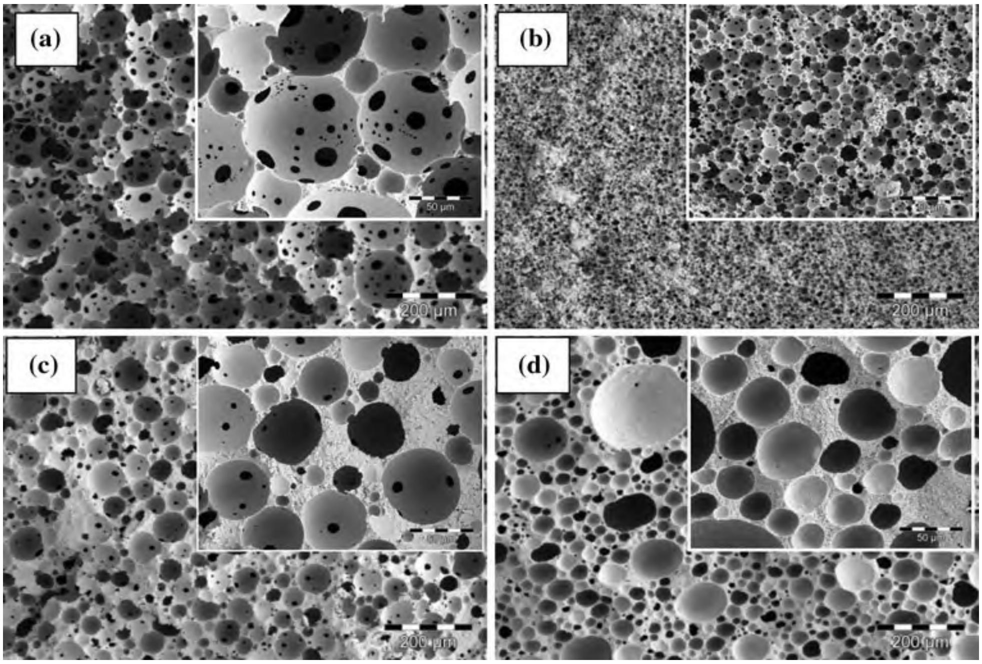

Fig. 6 SEM microstructures of sintered foams (1,550 °C for 2 h) produced from Su-Em of different compositions: **a** Su-Em-1, **b** Su-Em-2 and **c** Su-Em-3. In **d** Pa-Em-80% SiOH for comparison

Cellular ceramics produced from emulsified suspensions of similar composition and processing conditions, stabilized either by surfactant molecules or by colloidal particles, can be seen in Fig. 6b, d, respectively. The Pa-Em based foams present larger cells and thicker struts with a wider size distribution than the Su-Em based material. As no foaming is observed in the particle-stabilized systems, the larger cells are a result of larger droplets formed during emulsification. The fragmentation of the dispersed phase depends mainly on the ratio between the shear and interfacial stresses applied during shearing [30]. Larger droplets in Pa-Em are the result of higher interfacial tensions compared with the surfactant-stabilized case. Further on, as the surfactant-stabilized bubbles grow during foaming, the resulting solids can have a higher porosity than in the case of particle stabilization. Cellular ceramics with similar porosity parameters, namely a porosity of 60.7% or 63.9, a cell size of 27.6 or 24.5 µm and a strut thickness of 2.4 or 3.0 µm could be achieved using Su-Em-3 or Pa-Em-80% SiOH-based systems, respectively.

A remarkable difference between the Su-Em and Pa-Em based cellular materials is the interconnectivity between cells (Fig. 6). The presence of thin surfactant films connecting two bubbles in the wet stage and the subsequent expansion of bubbles easily provide windows between adjacent cells in Su-Em based materials. In particle-stabilized systems, windows can also be achieved. However, this is normally produced in systems containing a low concentration of particles or ones in which controlled coalescence occurs [25, 31].

The use of porous ceramics in extreme environments e.g., at high temperatures is more and more desirable. A high mechanical performance of the materials in the application field is demanded. In this context, the compressive strength at high temperature of cellular ceramics of similar porosity parameters achieved by surfactant or particle-stabilized systems has been determined. Closed-cell structures (as in the case of Pa-Em) are expected to have higher compressive strength than interconnected ones [32]. However, could it be that the particle stabilization on the droplets has further effects on the final cell properties? Preliminary tests show that the compression strength at 1,500 °C of the surfactant-stabilized material Su-Em-3 is up to 40 MPa whilst that of the particle-stabilized material Pa-Em-80% SiOH is even higher, up to 64 MPa. Thus, the particle-stabilized based materials are extremely stable under mechanical pressure at high temperature presenting constant geometries after the tests. These initial results highlight their potential in applications with intense thermal and mechanical requirements.

The thermal properties of the cellular ceramics are very important for their use at high temperatures. Controlled thermal isolation and the presence of temperature gradients are, for example, a result of the materials' thermal properties. The thermal diffusivity of surfactant and particle-stabilized based materials as a function of temperature is

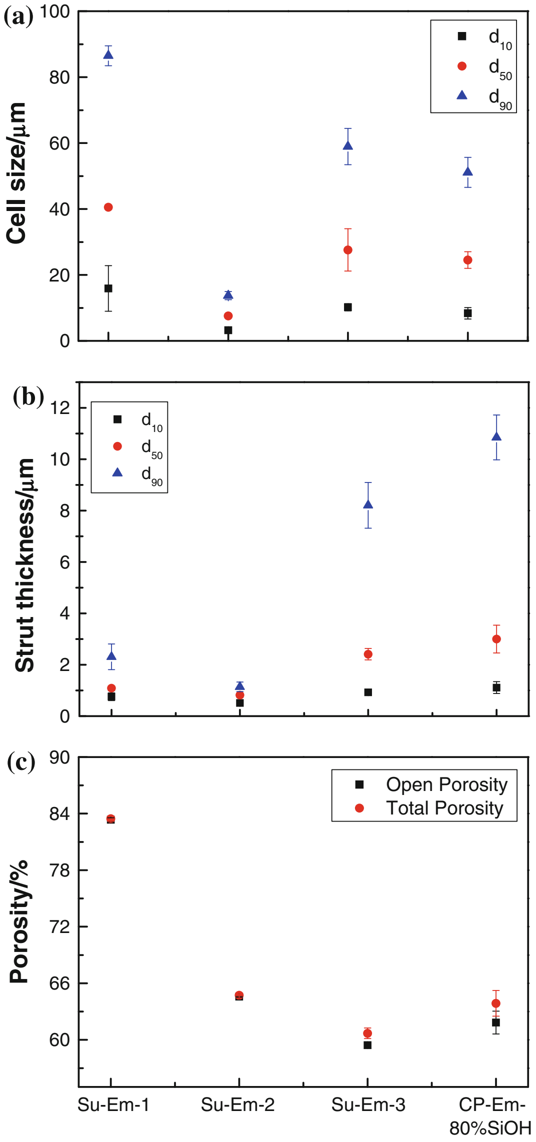

Fig. 7 Porosity parameters of sintered foams of Su-Em. **a** Cell size, **b** strut thickness, **c** total and open porosities for different conditions. The porosity parameters of foams produced from Pa-Em with SiO_2 particles containing 80% residual SiOH are presented for comparison

depicted in Fig. 8. The diffusivity strongly depends on the temperature so that the materials become more isolating at high temperatures. Particle stabilization and the presence of closed cells (without windows between them) do not seem to result in an extra effect in the diffusivity of the materials. Besides the environment temperature, the material porosity seems to be an important parameter. At 25 °C, the diffusivity can be 6.9 mm^2/s for 60.7% porosity (Su-Em-3) or 4.7 mm^2/s for 83.4% porosity (Su-Em-1). The porosity dependence vanishes with an increase in temperature. At 1,000 °C the diffusivity reaches the lowest values ranging between 0.9 and 0.7 mm^2/s for the different compositions tested.

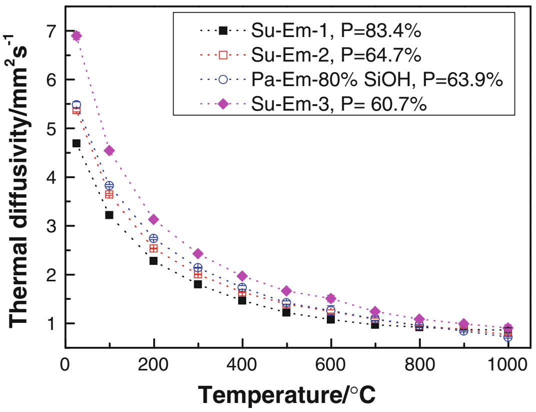

Fig. 8 Thermal diffusivity from 25 to 1,000 °C of cellular ceramics produced from surfactant and nanoparticle-stabilized emulsified suspensions. The porosity P is included

4 Conclusions

Emulsified alumina particle suspensions containing homogeneously dispersed oil droplets stabilized by aggregates of silica nanoparticles and alumina microparticles have been successfully prepared. Varying the residual SiOH content on silica particle surfaces between 80 and 15% resulted in very stable emulsified suspensions where neither coalescence nor subsequent bubble growth occurred. Emulsified suspensions with oil-in-water morphology have been prepared for a range of silica particle wettabilities, from very hydrophobic (15% SiOH) to very hydrophilic particles (100% SiOH). The solid materials after setting and sintering presented open porosities between 49 and 61% and average cell sizes between 17.7 and 25.4 µm. By contrast, surfactant-stabilized emulsified suspensions exhibited bubble growth during foaming leading to higher porosities (up to 83%) and interconnected cells.

The developed materials displayed remarkable compressive strength at 1,500 °C, being up to 40 and 64 MPa for surfactant and particle-stabilized based systems, respectively. Thermal diffusivity as low as 0.7 mm^2/s can be reached at 1,000 °C. These preliminary results highlight the potential of purely particle-based ceramics for applications in extreme environments.

Acknowledgments The authors would like to thank DFG for funding this project within the Research Training Group 1375 ''Nonmetallic Porous Structures for Physical–Chemical Functions'' and Wacker-Chemie (Germany) for the supply of the fumed silica powders.

References

1. S.M.H. Olhero, J.M.P.Q. Delgado, J.M.F. Ferreira, C. Pinho, Development of porous ceramics for gas burners. Defect Diffus. Forum **273–276**, 814–819 (2008)

2. N.L. de Freitas, J.A.S. Goncalves, M.D.M. Innocentini, J.R. Coury, Development of a double-layered ceramic filter for aerosol filtration at high-temperatures: The filter collection efficiency. J. Hazard. Mater. **136**(3), 747–756 (2006)
3. L.L. Hench, J. Wilson (eds.), *Introduction to Bioceramics* (World Scientific, Singapore, 1993)
4. J.-F. Drillet, M. Adam, S. Barg, A. Herter, D. Koch, V. Schmidt, M. Wilhelm, Development of a novel zinc/air fuel cell with a Zn foam anode, a PVA/KOH membrane and a MnO[sub 2]/SiOC-based air cathode. ECS Trans. **28**(32), 13–24 (2010)
5. E.M.M. Ewais, S. Barg, G. Grathwohl, A.A. Garamoon, N.N. Morgan, Processing of open porous zirconia via alkane-phase emulsified suspensions for plasma applications. Int. J. Appl. Ceram. Technol. **8**(1), 85–93 (2011)
6. J. Hüppmeier, S. Barg, M. Baune, D. Koch, G. Grathwohl, J. Thöming, Oxygen feed membranes in autothermal steam-reformers—a robust temperature control. Fuel **89**(6), 1257–1264 (2010)
7. M. Scheffler, P. Colombo, *Cellular Ceramics: Structure, Manufacturing, Properties and Applications* (Wiley-VCH, Weinheim, 2005)
8. M. Pulkin, D. Koch, G. Grathwohl, Silica effect on porous calcium phosphate ceramics from the freeze gelation route. Int. J. Appl. Ceram. Technol. (in press, corrected proof)
9. S. Barg, M.D.M. Innocentini, R.V. Meloni, W.S. Chacon, H. Wang, D. Koch, G. Grathwohl, Physical and high-temperature permeation features of double-layered cellular filtering membranes prepared via freeze casting of emulsified powder suspensions. J. Membr. Sci. **383**, 35–43 (2011)
10. A.R. Studart, U.T. Gonzenbach, E. Tervoort, L.J. Gauckler, Processing routes to macroporous ceramics: A review. J. Am. Ceram. Soc. **89**(6), 1771–1789 (2006)
11. P. Colombo, Conventional and novel processing methods for cellular ceramics. Philos. Trans. R. Soc. A Math. Phys. Eng. Sci. **364**(1838), 109–124 (2006)
12. A. Imhof, D.J. Pine, Ordered macroporous materials by emulsion templating. Nature **389**(6654), 948–951 (1997)
13. C. Solans, J. Esquena, N. Azemar, Highly concentrated (gel) emulsions, versatile reaction media. Curr. Opin. Colloid Interface Sci. **8**(2), 156–163 (2003)
14. H. Zhang, G.C. Hardy, Y.Z. Khimyak, M.J. Rosseinsky, A.I. Cooper, Synthesis of hierarchically porous silica and metal oxide beads using emulsion-templated polymer scaffolds. Chem. Mater. **16**(22), 4245–4256 (2004)
15. H.F. Zhang, A.I. Cooper, Synthesis and applications of emulsion-templated porous materials. Soft Matter **1**(2), 107–113 (2005)
16. S. Barg, C. Soltmann, M. Andrade, D. Koch, G. Grathwohl, Cellular ceramics by direct foaming of emulsified ceramic powder suspensions. J. Am. Ceram. Soc. **91**(9), 2823–2829 (2008)
17. S. Barg, E.G. de Moraes, D. Koch, G. Grathwohl, New cellular ceramics from high alkane phase emulsified suspensions (HAPES). J. Eur. Ceram. Soc. **29**(12), 2439–2446 (2009)
18. S. Barg, D. Koch, G. Grathwohl, Processing and properties of graded ceramic filters. J. Am. Ceram. Soc. **92**(12), 2854–2860 (2009)
19. S. Barg, Cellular ceramics via alkane phase emulsified powder suspensions, PhD Thesis in *Production Engineering* (University of Bremen, Bremen, 2010)
20. S.U. Pickering, J. Chem. Soc. **91**, 2001–2021 (1907)
21. A. Menner, R. Verdejo, M. Shaffer, A. Bismarck, Particle-stabilized surfactant-free medium internal phase emulsions as templates for porous nanocomposite materials: Poly-pickering-foams. Langmuir **23**(5), 2398–2403 (2007)
22. V.O. Ikem, A. Menner, A. Bismarck, High internal phase emulsions stabilized solely by functionalized silica particles. Angew. Chem. **120**(43), 8401–8403 (2008)
23. N. Brun, S. Ungureanu, H. Deleuze, R. Backov, Hybrid foams, colloids and beyond: From design to applications. Chem. Soc. Rev. **40**(2), 771–788 (2011)
24. B.P. Binks, Macroporous silica from solid-stabilized emulsion templates. Adv. Mater. **14**(24), 1824–1827 (2002)
25. I. Aranberri, B.P. Binks, J.H. Clint, P.D.I. Fletcher, Synthesis of macroporous silica from solid-stabilised emulsion templates. J. Porous Mater. **16**(4), 429–437 (2009)
26. I. Akartuna, A.R. Studart, E. Tervoort, U.T. Gonzenbach, L.J. Gauckler, Stabilization of oil-in-water emulsions by colloidal particles modified with short amphiphiles. Langmuir **24**(14), 7161–7168 (2008)
27. I. Akartuna, A.R. Studart, E. Tervoort, L.J. Gauckler, Macroporous ceramics from particle-stabilized emulsions. Adv. Mater. **20**(24), 4714 (2008)
28. M. Cerbelaud, A. Videcoq, P. Abelard, C. Pagnoux, F. Rossignol, R. Ferrando, Heteroaggregation between Al2O3 submicrometer particles and SiO2 nanoparticles: Experiment and simulation. Langmuir **24**(7), 3001–3008 (2008)
29. B.P. Binks, S.O. Lumsdon, Catastrophic phase inversion of water-in-oil emulsions stabilized by hydrophobic silica. Langmuir **16**(6), 2539–2547 (2000)
30. G.I. Taylor, The formation of emulsions in definable fields of flow, in *Proceedings of the Royal Society of London. Series A, Containing Papers of a Mathematical and Physical Character*, vol. 146, no. 858 (1934), pp. 501–523
31. U.T. Gonzenbach, A.R. Studart, E. Tervoort, L.J. Gauckler, Macroporous ceramics from particle-stabilized wet foams. J. Am. Ceram. Soc. **90**(1), 16–22 (2007)
32. L.J. Gibson, M.F. Ashby, *Cellular Solids: Structure & Properties* (Cambridge University Press, Cambridge, 1997)